Journal of the Brazilian Society of Mechanical Sciences and Engineering
Print ISSN 1678-5878

J. Braz. Soc. Mech. Sci. & Eng. vol.25 no.2 Rio de Janeiro Apr./ June 2003

Application of mass conservation method to investigate the wind patterns over an area of complex topography

H. A. Karam; A. P. Oliveira; J. Soares

Group of Micrometeorology, Department of Atmospheric Science, IAG University of São Paulo, Rua do Matão, 1226, 05508-900 São Paulo, SP. Brazil. apdolive@usp.br, jacyra@usp.br

---

ABSTRACT

The most basic mass conservation method is described here in detail. A simplified version of this method is then applied to estimate the wind field over a region of complex topography, the Metropolitan Region of São Paulo City, Brazil. The resulting adjusted wind field and its horizontal divergence patterns compare well with observed wind field, indicating that the topography has a major effect in the investigated area.

Keywords: Wind field over complex terrain, mass conservation method, São Paulo City

Introduction

The appropriate description of wind field over complex terrain is important to prognostic correctly the temporal and spatial evolution of airborne pollutant.

Operationally the wind field can be estimated by interpolating observed values at surface and/or from vertical soundings (Goodin *et al.*, 1979 and 1981; Maddox, 1980; Kock *et al.*, 1983). Despite its very low computational cost, this procedure usually presents errors due to inadequate instrumentation exposure, deficient calibration and lack of spatial resolution. These errors are particularly important over regions of complex topography.

Alternatively, the wind field can be obtained from numerical simulation using numerical models with horizontal resolution of 1 km or even smaller such as the Fifth-Generation NCAR/Penn State Mesoscale Model (MM5), Regional Atmospheric Mesoscale Model (RAMS), and Three-dimensional Vorticity Model (TVM) etc. In spite of their physical capability, running mesoscale models in a regular basis has a large computational cost. Besides, lack of observation in high spatial resolution precludes an appropriate specification of boundary and initial conditions, reducing considerably the performance of numerical simulations.

A method that compromises simple interpolation routine with physical constraints will be explored in this paper. In this technique the effect of topography is estimated imposing mass conservation to the observed wind field (Dickerson, 1978; Sherman, 1978). Compared to simple interpolation scheme, this method is superior because it incorporates a physical constraint - mass conservation. Compared to mesoscale models, this method has a much lower computational cost and therefore, it can be used routinely to estimate wind field for a broad range of applications (Endlich *et al.*, 1982; Moussiopoulos and Flassak, 1986; Durran, 1990).

In this work, the most basic mass conservation method is described in detail in order to clarify derivation procedure, which has not been explicitly addressed in the literature. A simplified version of this method is then applied to estimate the

wind field over a region of complex topography, the Metropolitan Region of São Paulo City, Brazil. The resulting adjusted wind field and its horizontal divergence pattern are compared to observed wind field.

Investigated Area

The wind field will be estimated in the northern portion of the Metropolitan Region of São Paulo (Figure 1). The central point of this area corresponds to $23^0$33'35''S and $46^0$43'55"W. The main topographic features are the valleys of: Tietê River, oriented in the east-west direction; Pinheiros River and Tamanduateí River both oriented in the south-north direction. The high elevation seen in the northeast of this domain corresponds to Cantareira Mountain with crests up 1000 meters.

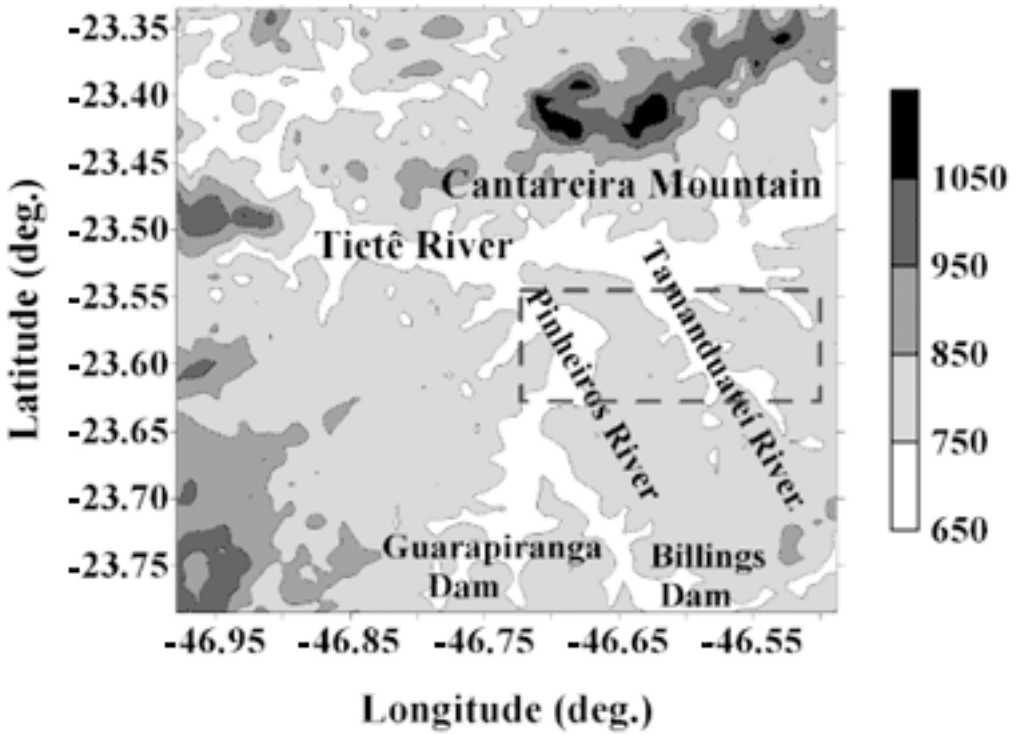

Figure 1. Topographic features of northern portion of the Metropolitan Region of São Paulo (50 by 50 km). The contour gray-scales represent the topographic levels (in meter). The small rectangle represents the observation domain.

The small rectangle shown in Figure 1 represents the region of the domain where there are wind field observations utilized in a previous study (Oliveira *et al.*, 2003). This region, hereafter, will be called "observation domain".

Observed Wind Field Over the City of São Paulo

According to Oliveira *et al.* (2003), the wind hodograph pattern over the observation domain has an elliptical shape in almost all months. The wind hodograph and the diurnal evolution of the wind speed - both averaged over the observation domain - are displayed, respectively, in Figures 2 and 3, for April 1988. Figure 4 shows the diurnal evolution of the wind field divergence over the observation domain also for April 1988. According to the authors the pattern, seen in Figure 4, is caused by the combination of sea breeze and topographic effects in the São Paulo City area.

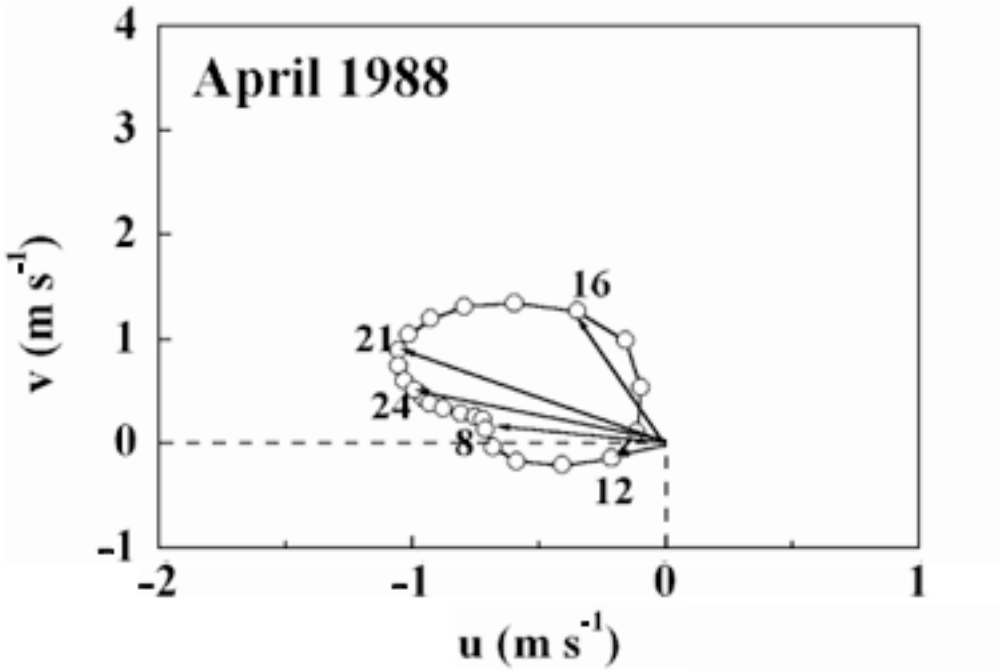

Figure 2. Hodograph of the observed wind field, averaged over the observation domain for April 1988 (from Oliveira *et al.*, 2003). The numbers indicate local time.

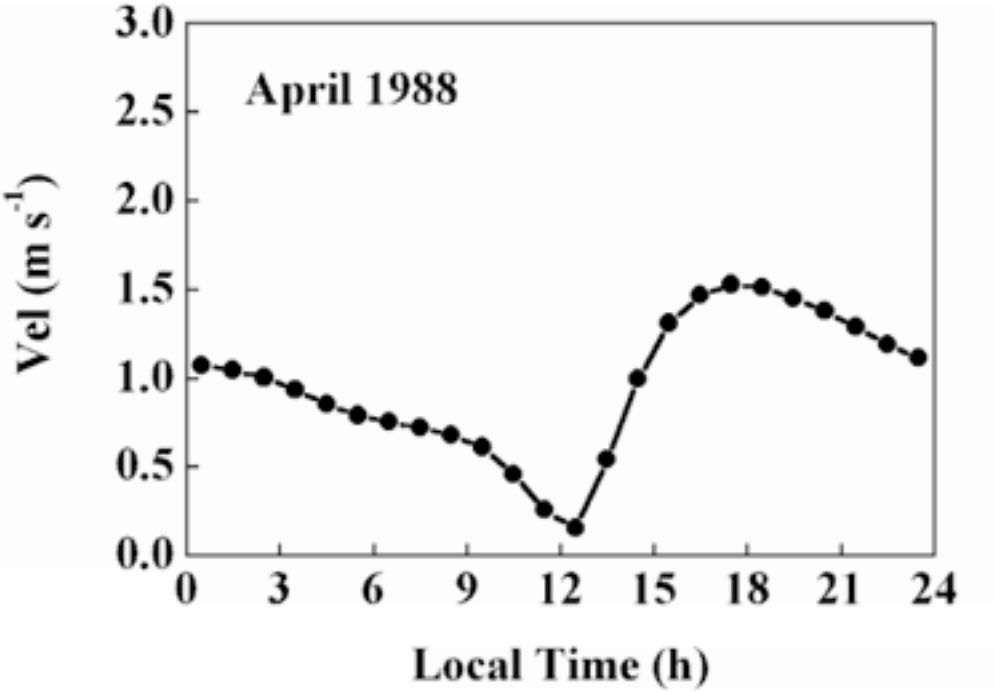

Figure 3. Diurnal evolution of the observed horizontal wind speed, averaged over the observation domain for April 1988 (from Oliveira *et al.*, 2003).

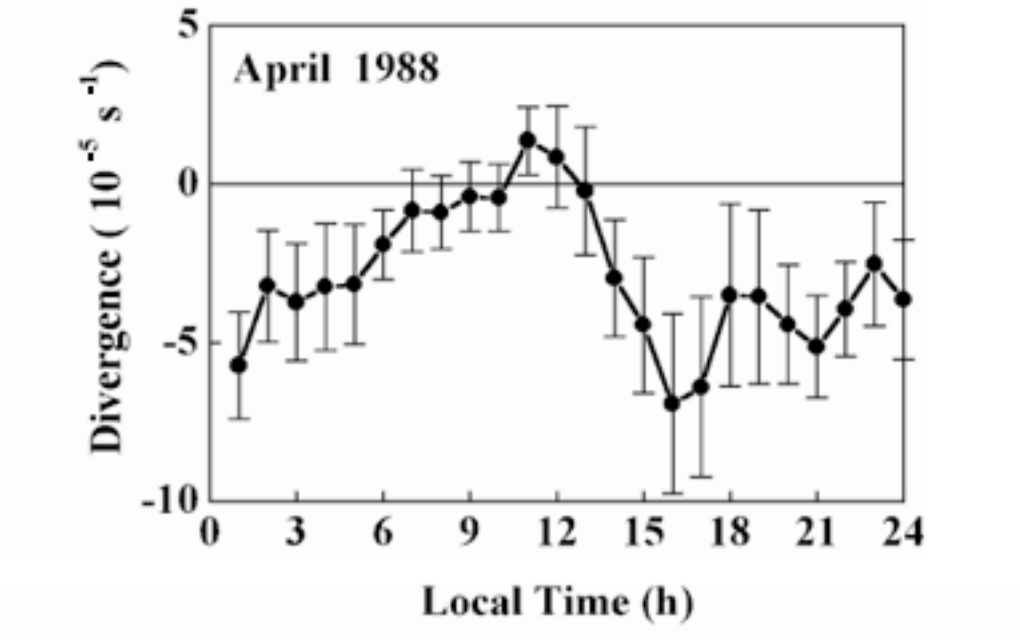

Figure 4. Diurnal evolution of the observed horizontal wind field divergence, averaged over the observation domain for April 1988. The bars represent the errors (from Oliveira *et al.*, 2003).

Mass Conservation Method

Reynolds-averaged wind field can be considered non-divergent when the scales of turbulent motions in the planetary boundary layer (PBL) are taking into consideration (Dutton, 1986). Therefore, $\partial \overline{u}/\partial x + \partial \overline{v}/\partial y + \partial \overline{w}/\partial z = 0$ is a valid approximation for the mass continuity equation, where $(\overline{u}, \overline{v}, \overline{w})$ are zonal, meridional and vertical components of Reynolds-averaged values of the actual wind field and x, y and z are, respectively, zonal, meridional and vertical directions. The Reynolds averages are indicated by bars over the symbols

Regardless the interpolation scheme, there is no guarantee that the interpolated wind field ($\overline{\vec{v}}^0$) obeys the mass conservation law described above. Wind field divergence is usually different from zero ($\nabla.\overline{\vec{v}}^0 \neq 0$) as result of (i) measurement errors; (ii) lack of spatial resolution and (iii) numerical errors inherent in any interpolation scheme. Errors (i) and (ii) are particularly important in areas with complex topography.

To overcome this inconsistency it is hypothesized that the difference between the actual and interpolated wind field is induced only by the topography. Expressing this difference by $\overline{\vec{c}} = \overline{\vec{v}} - \overline{\vec{v}}^0$, the mass conservation in the PBL can be rewritten as:

$$\nabla.\overline{\vec{c}} = -\nabla.\overline{\vec{v}}^0 \qquad (1)$$

where: $\overline{\vec{c}} = \overline{u}^c\,\vec{i} + \overline{v}^c\,\vec{j} + \overline{w}^c\,\vec{k}$, is the correction; $\overline{\vec{v}} = \overline{u}\,\vec{i} + \overline{v}\,\vec{j} + \overline{w}\,\vec{k}$ the actual wind and $\overline{\vec{v}}^0 = \overline{u}^0\,\vec{i} + \overline{v}^0\,\vec{j} + \overline{w}^0\,\vec{k}$ the initial guess or interpolated wind field.

Assuming that the correction can be expressed in terms of the gradient of a potential function, (1) can be written as:

$$\nabla^2\overline{\phi} = -\nabla.\overline{\vec{v}}^0 \qquad (2)$$

This equation can be solved numerically, for a given interpolated wind field $\overline{\vec{v}}^0(x, y, z)$ and appropriated boundary conditions for $\overline{\phi}(x,y,z)$, so that the actual wind field can be estimated as:

$$\{\overline{u}, \overline{v}, \overline{w}\} = \left\{\overline{u}^0 + \frac{\partial\overline{\phi}}{\partial x},\ \overline{v}^0 + \frac{\partial\overline{\phi}}{\partial y},\ \overline{w}^0 + \frac{\partial\overline{\phi}}{\partial z}\right\} \qquad (3)$$

where $(\overline{u}^0, \overline{v}^0, \overline{w}^0)$ are the zonal, meridional and vertical components of the

interpolated wind field ($\vec{\bar{v}}^0$) in a regular grid. In general it is assumed that $\bar{\phi}$ =0 at the boundaries (Brocchini *et al*., 1995).

Unfortunately, the wind observations are routinely available only in one, or few more, point at the surface, making necessary to interpolate the wind field for the rest of domain in order to apply equations (2) and (3). The lack of vertical wind field information is even more critical but it can only be overcome by vertically averaging equation (2):

$$\frac{1}{(h - z_S)} \int_{z_S}^{h} \nabla^2 \bar{\phi} \, dz = -\frac{1}{(h - z_S)} \int_{z_S}^{h} \nabla . \vec{\bar{v}}^0 \, dz \qquad (4)$$

where z_S is the wind measurement level ($z_S = z_g + 10$ m) and z_g is the surface height.

The topographic adjustment depth (h) has several equivalent definitions in the literature. For instance, Dickerson (1978) defined h as the height of the mixed layer. On the other hand, Ross and Fox (1991) defined h as a characteristic height associated to the topographic elements of the terrain. Ludwig *et al.* (1991) defined h as the height where the work done against the buoyant restoring force equals the kinetic energy as the surface flow parcels are displaced vertically by the topographic elements. This last definition allows to estimate h as:

$$h = V_S / N_B \qquad (5)$$

where V_S is the observed horizontal wind speed magnitude at the reference level, and N_B the Brunt-Väisälä frequency. In this work h will be given by the Ludwig *et al.* (1991) definition and estimated from (5).

Defining the vertically average value of a function f as $\langle f \rangle = (h - z_S)^{-1} \int_{z_S}^{h} f \, dz$, equation (4) can be written as:

$$\nabla_H^2 \langle \bar{\phi} \rangle = -(h - z_S)^{-1} \left\{ \nabla_H . \left[\left(h - z_S \right) \langle \vec{\bar{v}}_H^0 \rangle \right] \right\} + \varepsilon \qquad (6)$$

where $\nabla_H = \frac{\partial}{\partial x} \vec{i} + \frac{\partial}{\partial y} \vec{j}$, $\vec{\bar{v}}_H^0 = \bar{u}^0 \vec{i} + \bar{v}^0 \vec{j}$ and the contribution due to vertical structure of the wind (ε):

$$\varepsilon = -(h - z_S)^{-1}\left\{ \left[2\nabla_H \langle \bar{\phi} \rangle \cdot \nabla_H (h - z_S) + \langle \bar{\phi} \rangle \nabla_H^2 (h - z_S) \right] \right.$$
$$- \left[2\nabla_H h \cdot \nabla_H \bar{\phi}(h) + \bar{\phi}(h) \nabla_H^2 h - \frac{\partial \bar{\phi}(h)}{\partial z} \right]$$
$$+ \left[2\nabla_H z_S \cdot \nabla_H \bar{\phi}(z_S) + \bar{\phi}(z_S) \nabla_H^2 z_S - \frac{\partial \bar{\phi}(z_S)}{\partial z} \right]$$
$$- \left[\bar{\vec{v}}_H^0(h) \cdot \nabla_H h - \bar{w}^0(h) \right]$$
$$\left. + \left[\bar{\vec{v}}_H^0(z_S) \cdot \nabla_H z_S - \bar{w}^0(z_S) \right] \right\} \qquad (7)$$

with $\bar{\phi}(z_S) = \bar{\phi}(x, y, z_S)$ and $\bar{\phi}(h) = \bar{\phi}(x, y, h)$. The details about the derivation of equations (6) and (7) are given in Appendixes A, B and C.

Equation (6) is the complete version of continuity equation averaged vertically through the topographic adjustment layer. As far as the authors are aware this equation version is not available in the literature.

The most known simplified version of equation (6), used in several applications (Anderson, 1971; Dickerson, 1978) and utilized also in this work, is:

$$\nabla_H^2 \langle \bar{\phi} \rangle = -(h - z_S)^{-1} \left\{ \nabla_H \cdot \left[(h - z_S) \langle \bar{\vec{v}}_H^0 \rangle \right] \right\} \qquad (8)$$

The correction resulting from the equation (8)corresponds to:

$$\{ \langle \bar{u} \rangle, \langle \bar{v} \rangle, \langle \bar{w} \rangle \} = \left\{ \langle \bar{u}^0 \rangle + \frac{\partial \langle \bar{\phi} \rangle}{\partial x}, \langle \bar{v}^0 \rangle + \frac{\partial \langle \bar{\phi} \rangle}{\partial y}, \langle \bar{w}^0 \rangle \right\} \qquad (9)$$

Expression (7) contains all the terms that have to be summed to zero in order to eliminate the error when (8) is applied to estimate the correction for the vertically average wind speed that is adjusted to the topography.

The error indicated in the expression (7) can not be completely estimate for real flows, because it depends $\bar{\phi}$ and interpolated (initial) flow at the boundaries of the domain, which are not available. However, the error given by (7), can be minimized by considering a constant topographic adjustment depth as it was done here. In this case all spatial derivatives of h in (7) are equal to zero and the remaining terms will be a function of the topography.

Numerical Solution

Equation (8) was written using finite-difference on a regular grid and its solution was obtained using a two-dimensional *Black and RedSequential Over-Relaxation* routine (Press *et al.*, 1992). $\langle \overline{\Phi} \rangle = 0$ was considered as boundary condition (Brocchini *et al.* 1995). The used grid has 100 by 100 points distributed over an area of 50 by 50 km. The grid resolution corresponds to the topography resolution (500 m).

The topographic adjustment depth was set constant and equal to 150 meters. This value was obtained from expression (5), considering as typical value for the horizontal wind speed magnitude at the reference level (V_S) the averaged value for April 1988 (Figure 3), 1.1 m s^{-1}, and for the Brunt-Väisälä frequency N_B ~ 0.008 s^{-1}. The N_B corresponds to a value of potential temperature vertical gradient of ~ 2 K km^{-1}, typically observed in the morning periods in the region of São Paulo city during April (Oliveira and Dias, 1982).

It was assumed that the wind field, used as input in the mass conservation method, has a diurnal evolution pattern with elliptical shape (Figure 5, dashed line) similar to the averaged wind observed in the area of São Paulo City (Figure 2). The corresponding input wind intensity can be seen in Figure 6 (dashed line). In these figures are also displayed the adjusted wind field averaged over the observation domain (continuous lines). The largest difference between input and adjusted wind fields occurs during nighttime (18-03 LT).

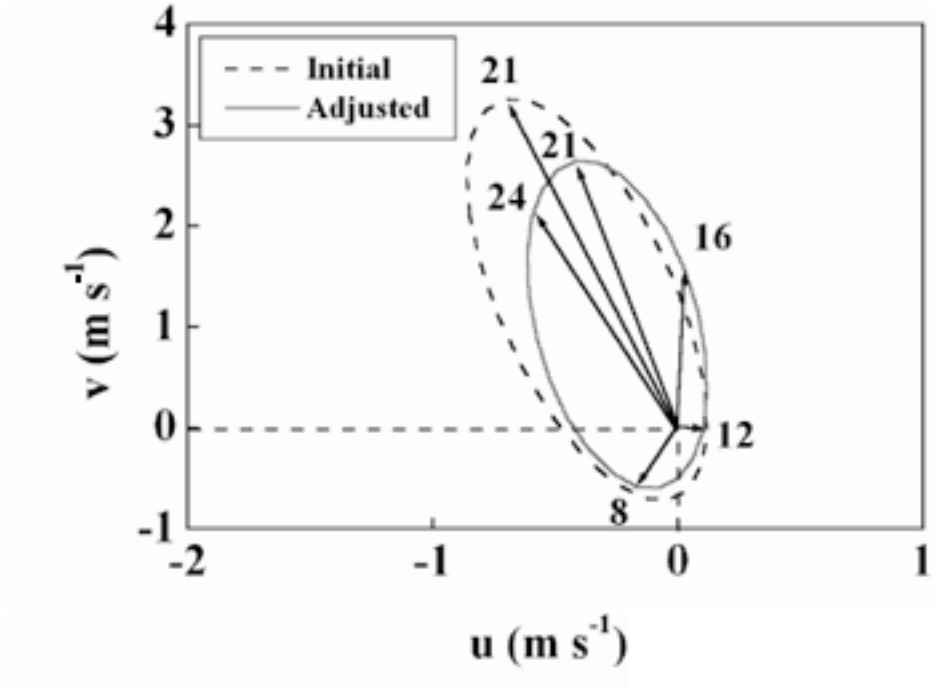

Figure 5. Input (dashed line) and adjusted (continuous line) wind hodographs. The numbers indicate local time.

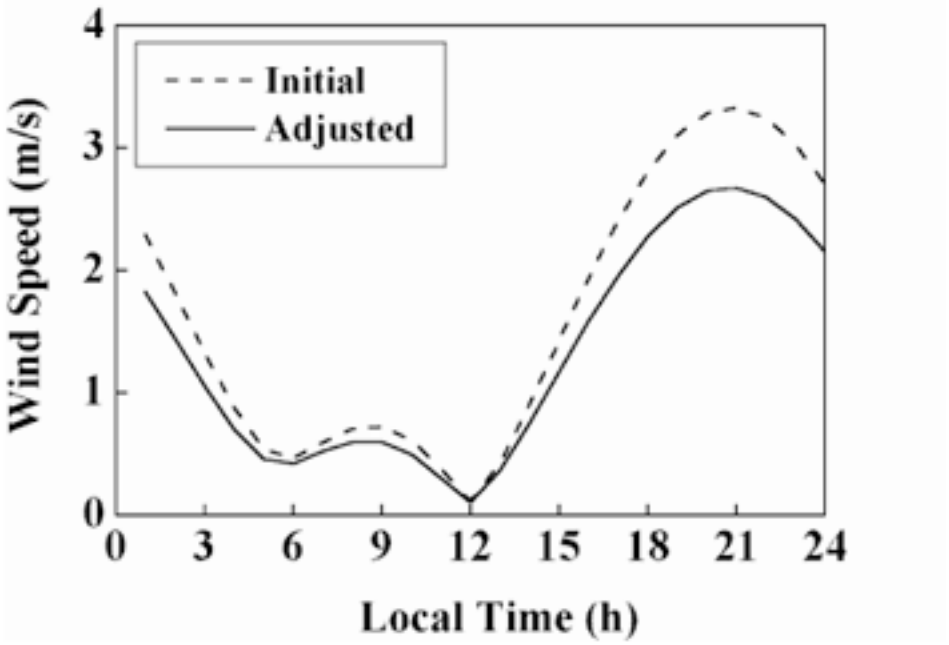

Figure 6. Diurnal evolution of the input (dashed line) and adjusted (continuous line) wind speed, averaged over the observation domain.

The diurnal evolution of the horizontal wind divergence obtained from the adjusted wind field over the observation domain (Figure 7) is similar to the observed one (Figure 4). During the morning the area is dominated by an incipient divergence followed by stronger convergence in the rest of the period. This pattern is also present in the observed wind field in São Paulo. The maximum convergence occurs around 21 LT and around 16 LT, respectively for adjusted and observed wind field.

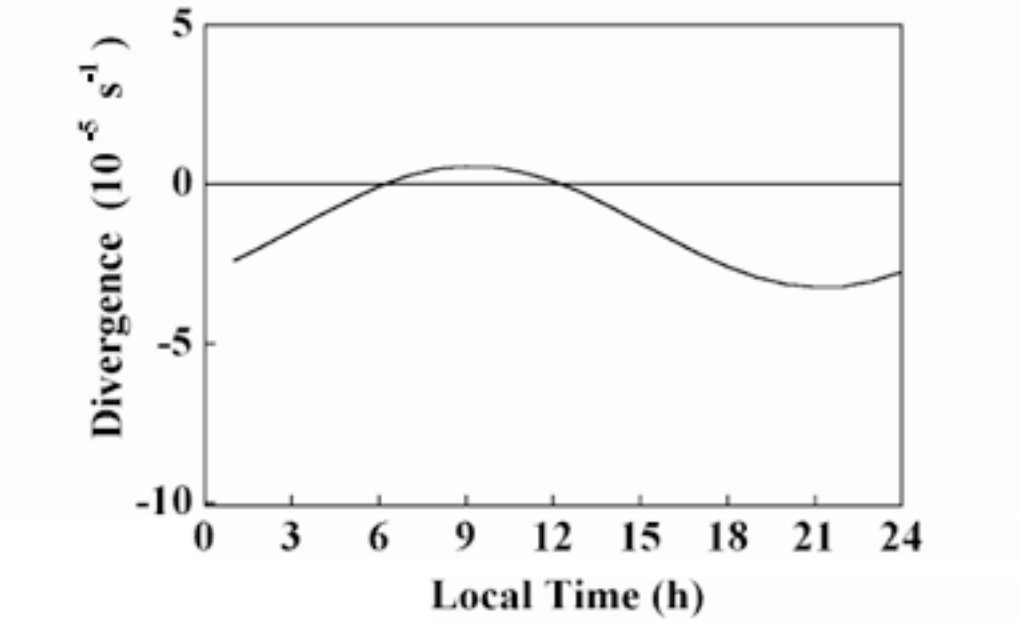

Figure 7. Diurnal evolution of the adjusted horizontal wind field divergence, averaged over the observation domain.

The maximum convergence at 21 LT, displayed in Figure 7, can be explained by blocking effects caused by large scale features of the topography (see Cantareira Mountains in Figure 8). At this time the adjusted wind flow is from South, flowing against the Cantareira Mountains. This large scale topographic effect can also explain the adjusted horizontal wind divergence observed during morning hours, when the wind is from North.

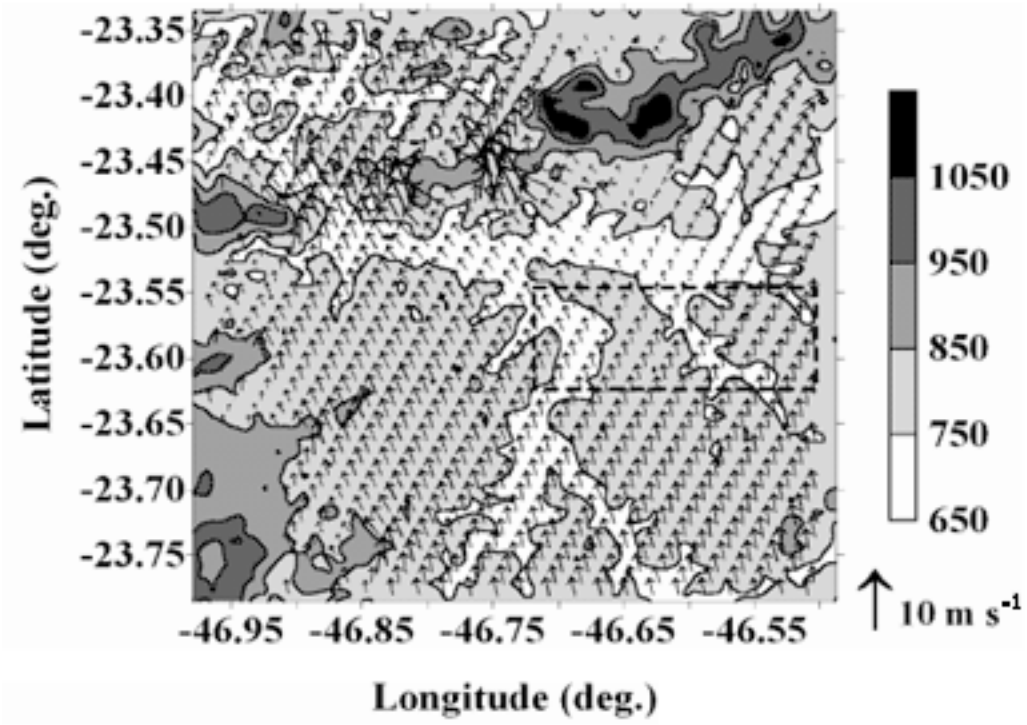

Figure 8. Adjusted wind field, at 21 LT, on the Metropolitan Region of São Paulo. The contour gray-scales represent the topographic levels (in meter).

The small scale topographic features contribute also to the diurnal evolution of divergence in the observation domain (Figure 7). The adjusted wind field, displayed in Figure 9, responds to small valleys and hills in the observation domain. This small scale blocking effect is clearly observed in the spatial distribution of the horizontal divergence (Figure 10).

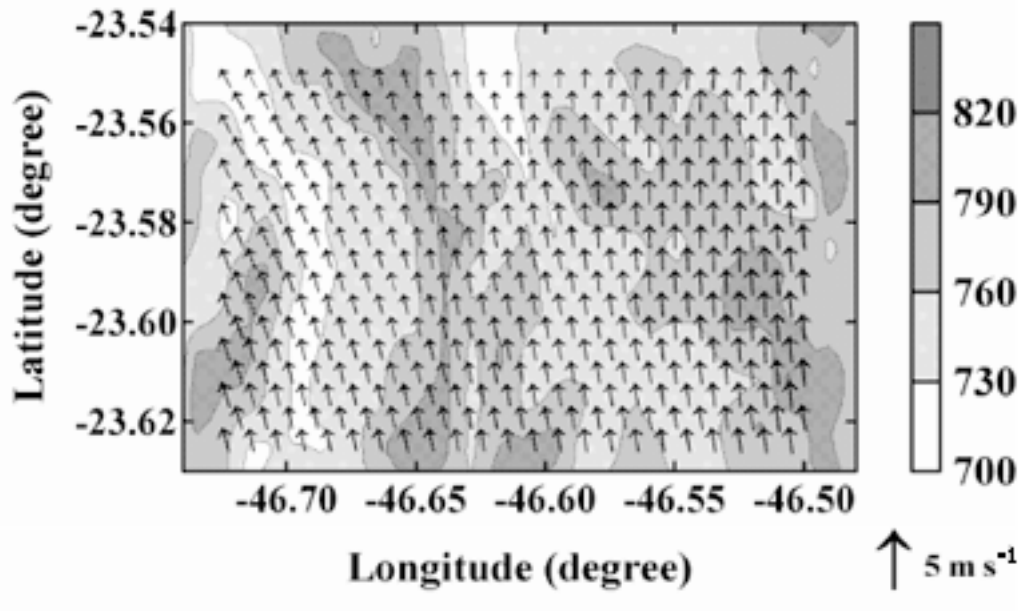

Figure 9. Adjusted wind field, at 21 LT, on the observation domain. The contour gray-scales represent the topographic levels (in meter).

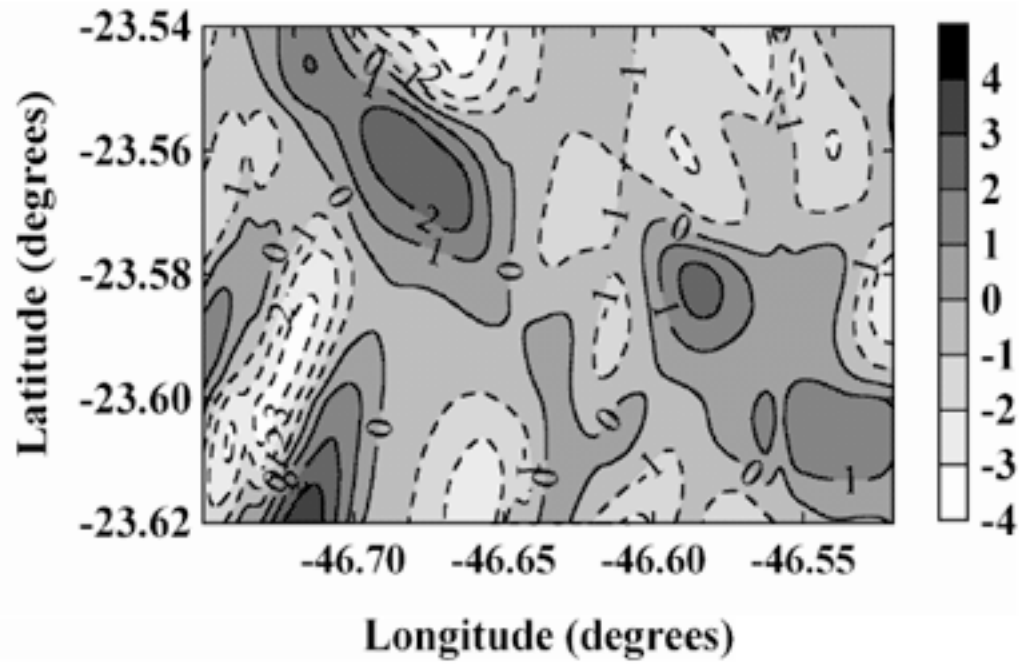

Figure 10. Adjusted horizontal wind field divergence, at 21 LT, on the observation domain.

Discussion and Conclusions

The derivation of mass conservation method described here indicates that simplified version of this method (eqs. 8 and 9) has an error that depends on: (i) the observed wind field vertical structure; (ii) the spatial variation of the topographic adjustment depth; (iii) curvature of topography; (iv) vertical component of observed wind at the top of the topographic adjustment depth and at reference level. Unfortunately this error can not be evaluated for real flows. However, the assumption of a constant topographic adjustment depth, assumed in the applications carried out here, contributes to reduce this error.

A simplified version of this method was applied to estimate the wind field over the Metropolitan Region of São Paulo City. The results show that for h estimated from equation (5), the absolute value of the correction lies between 0 and 11 m s^{-1}, and the resulting wind field is strongly modulated by topography. Under this circumstance, the diurnal evolution of the adjusted wind field was similar to the averaged wind observed in the area of São Paulo City. The amplitude of the divergence signal was also comparable to the observed in São Paulo indicating that the simplified expression used here to estimate h is appropriated for the topography of the investigated area and for the observed meteorological conditions during April 1988.

The horizontal wind divergence obtained from the adjusted field indicates that both large and small features of topography have a major effect in this area. The divergence during morning hours and convergence in the rest of the period are present in the observed and adjusted wind fields, clearly indicating that the topography has a major effect in the wind behavior in São Paulo. The presence of Cantareira Mountains alters significantly the sea breeze circulation in São Paulo, blocking the northerly flow during the morning and the southerly flow in the rest of the period. The small scale topographic features contribute also to the diurnal evolution of divergence in the observation domain.

Acknowledgments

This research was supported by "Fundação de Amparo a Pesquisa do Estado de São Paulo" (FAPESP), Brazil, under Grant No. 97/02843-0. The second and third author thanks, respectively, grants 300561/91-1 and 300040/94-6 from CNPq/ Brazil.

References

Anderson, G.E., 1971, "Mesoscale Influences on Wind Fields", J. Appl. Meteor., Vol.10, pp. 377-386.

Brocchini, M., Wurtele, M, Umgiesser, G. and Zecchetto, S, 1995, "Calculation of Mass-Consistent Two-Dimensional Wind Field with Divergence Control", J. Appl. Meteor., Vol.34, pp. 2543-2555.

Dickerson, M.H., 1978, "MASCON: A Mass Consistent Atmospheric Flux Model for Regions with Complex Terrain", J. Appl. Meteor., Vol.17, pp. 241-253.

Durran, D.R., 1990, "Mountain Waves and Down Slope Winds", Chapter in Atmospheric Processes over Complex Terrain, Editor: Banta, R.M., American Meteorological Society, Meteorological Monographs, Vol.23 (45), pp. 59-81.

Dutton, J.A., 1986, "Dynamics of Atmospheric Motion (formerly The Ceaseless Wind)", Dover Publications Inc., New York, USA, 617 p.

Endlich, R.M.; Ludwig, F.L. and Bhumralkar, C.M., 1982, "A Diagnostic Model for Estimating Winds at Potential Sites for Wind Turbines", J. Appl. Meteor., Vol.21, pp. 1441-1454.

Goodin, W.R.; McRae, G.J. and Seinfeld, J.H., 1979, "A Comparison of Interpolation Methods for Sparse Data: Application to Wind and Concentration Fields", J. Appl. Meteor., Vol.18, pp. 761-771.

Goodin, W.R.; McRae, G.J. and Seinfeld, J. H., 1981, "A Comparison of Interpolation Methods for Sparse Data: Application to Wind and Concentration Fields. Reply", J. Appl. Meteor., Vol.20, pp. 92-94.

Kock, S.E.; DesJardins, M. and Kocin, P.J., 1983, "An Interactive Barnes Objective Map Analysis Scheme for Use with Satellite and Conventional Data", J. Clim. Appl. Meteor., Vol.22 (10), pp. 1487-1502.

Ludwig, F.L.; Livingston, J.M. and Endlich, R.M., 1991, "Use of Mass Conservation and Critical Dividing Streamline Concepts for Efficient Objective Analysis of Winds in Complex Terrain", J. Appl. Meteor., Vol.30, pp. 1490-1499.

Maddox, R.A., 1980, "An Objective Technique for Separating Macroscale and Mesoscale Features in Meteorological Data", Mon. Wea. Rev., Vol.108, pp. 1108-1121.

Moussiopoulos, N. and Flassak, T., 1986, "Two Vectorized Algorithms for the Effective Calculation of Mass-Consistent Flow Fields", J. Climate Appl. Meteor., Vol.25, pp. 847-857.

Oliveira, A.P; Bornstein, R.D. and Soares, J., 2003, "Annual and Diurnal Wind

Patterns in the City of São Paulo", accepted for publication in the Water, Air & Soil Pollution, FOCUS (in press).

Oliveira, A.P. and Dias, P.L.S., 1982, "Aspectos Observacionais da Brisa Marítima em São Paulo", Proceedings of the II Congr. Brasil. Meteor., Pelotas, RS, Brazil, 18B22, October 1982, II, pp. 129-161 (in Portuguese).

Press, W.H.; Teukolsky, S.A. and Vetterling, W.T., 1992, "Numerical Recipes in FORTRAN – The Art of Scientific Computing", Cambridge University Press, New York, USA, 963 p.

Ross, D.G. and Fox, D.G., 1991, "Evaluation of an Air Pollution Analysis System for Complex Terrain", J. Appl. Meteor., Vol.30, pp. 909-923.

Sherman, C.A., 1978, "A mass-Consistent Model for Wind Fields over Complex Terrain", J. Appl. Meteor., Vol.17, pp. 312-319.

Smith, R.D., 1989, "Mountain-Induced Stagnation Points in Hydrostatic Flow", Tellus, Vol.41 A, pp. 270-274.

Paper accepted March, 2003
Technical Editor: Clóvis Raimundo Maliska

Appendix A

The right side of equation (4) can be written as

$$\left\langle \nabla . \vec{\bar{v}}^{0} \right\rangle = \left(h - z_S\right)^{-1} \int_{z_S(x,y)}^{h(x,y)} \nabla . \vec{\bar{v}}^{0} \, dz$$

$$= \left(h - z_S\right)^{-1} \left[\int_{z_S(x,y)}^{h(x,y)} \left(\nabla_H . \vec{\bar{v}}_H^{0} \right) dz + \int_{z_S(x,y)}^{h(x,y)} d\bar{w}^{0} \right] \qquad \text{(A1)}$$

Applying Leibnitz's rule to move the ∇_H outside of the integral, yields

$$(h-z_S)^{-1}\int_{z_S}^{h}\nabla.\vec{\overline{v}}^{0}\,dz$$

$$=(h-z_S)^{-1}\left[\nabla_H.\int_{z_S}^{h}\vec{\overline{v}}_H^{0}dz-\vec{\overline{v}}_H^{0}(h).\nabla_H h+\vec{\overline{v}}_H^{0}(z_S).\nabla_H z_S+\overline{w}^{0}(h)-\overline{w}^{0}(z_S)\right] \quad (A2)$$

Defining the vertically averaged value of the function f as $\langle f\rangle = (h - z_S)^{-1} \int_{z_S}^{h} f\,dz$ results in:

$$\left\langle\nabla.\vec{\overline{v}}^{0}\right\rangle = (h-z_S)^{-1}\left\{\nabla_H.\left[(h-z_S)\left\langle\vec{\overline{v}}_H^{0}\right\rangle\right]\right.$$

$$\left.-\left[\vec{\overline{v}}_H^{0}(h).\nabla_H h-\overline{w}^{0}(h)\right]+\left[\vec{\overline{v}}_H^{0}(z_S).\nabla_H z_S-\overline{w}^{0}(z_S)\right]\right\} \quad (A3)$$

Appendix B

The left side of equation (4) can be written as:

$$\left\langle\nabla^2\overline{\phi}\right\rangle = (h-z_S)^{-1}\int_{z_S(z,y)}^{h(x,y)}\nabla^2\overline{\phi} = (h-z_S)^{-1}\int_{z_S(x,y)}^{h(x,y)}\left(\frac{\partial^2\overline{\phi}}{\partial x^2}+\frac{\partial^2\overline{\phi}}{\partial y^2}+\frac{\partial^2\overline{\phi}}{\partial z^2}\right)dz \quad (B1)$$

Considering only the x-direction and applying the Leibnitz's rule:

$$\int_{z_S}^{h}\frac{\partial^2\overline{\phi}}{\partial x^2}\,dz=\int_{z_S}^{h}\frac{\partial}{\partial x}\left(\frac{\partial\overline{\phi}}{\partial x}\right)dz=\frac{\partial}{\partial x}\int_{z_S}^{h}\left(\frac{\partial\overline{\phi}}{\partial x}\right)dz-\frac{\partial\overline{\phi}(h)}{\partial x}\frac{\partial h}{\partial x}+\frac{\partial\overline{\phi}(z_S)}{\partial x}\frac{\partial z_S}{\partial x} \quad (B2)$$

Applying once more,

$$\int_{z_S}^{h} \frac{\partial^2 \bar{\phi}}{\partial x^2} dz = \frac{\partial}{\partial x}\left[\frac{\partial}{\partial x}\int_{z_S}^{h} \bar{\phi} dz - \bar{\phi}(h)\frac{\partial h}{\partial x} + \bar{\phi}(z_S)\frac{\partial z_S}{\partial x}\right] - \frac{\partial \bar{\phi}(h)}{\partial x}\frac{\partial h}{\partial x} + \frac{\partial \bar{\phi}(z_S)}{\partial x}\frac{\partial z_S}{\partial x} \quad \text{(B3)}$$

Resulting expression is

$$\int_{z_S}^{h} \frac{\partial^2 \bar{\phi}}{\partial x^2} dz = \frac{\partial^2}{\partial x^2}\int_{z_S}^{h} \bar{\phi} dz + \left[-\frac{\partial \bar{\phi}(h)}{\partial x}\frac{\partial h}{\partial x} + \frac{\partial \bar{\phi}(z_S)}{\partial x}\frac{\partial z_S}{\partial x}\right] + \left[-\bar{\phi}(h)\frac{\partial^2 h}{\partial x^2} + \bar{\phi}(z_S)\frac{\partial^2 z_S}{\partial x^2}\right] - \frac{\partial \bar{\phi}(h)}{\partial x}\frac{\partial h}{\partial x} + \frac{\partial \bar{\phi}(z_S)}{\partial x}\frac{\partial z_S}{\partial x} \quad \text{(B4)}$$

For the three directions

$$\int_{z_S}^{h} \frac{\partial^2 \bar{\phi}}{\partial x^2} dz = \frac{\partial^2}{\partial x^2}\int_{z_S}^{h} \bar{\phi} dz - 2\left[\frac{\partial \bar{\phi}(h)}{\partial x}\frac{\partial h}{\partial x} - \frac{\partial \bar{\phi}(z_S)}{\partial x}\frac{\partial z_S}{\partial x}\right] - \left[\bar{\phi}(h)\frac{\partial^2 h}{\partial x^2} - \bar{\phi}(z_S)\frac{\partial^2 z_S}{\partial x^2}\right] \quad \text{(B5)}$$

$$\int_{z_s}^{h} \frac{\partial^2 \bar{\phi}}{\partial y^2} dz = \frac{\partial^2}{\partial y^2}\int_{z_s}^{h} \bar{\phi} dz - 2\left[\frac{\partial \bar{\phi}(h)}{\partial y}\frac{\partial h}{\partial y} - \frac{\partial \bar{\phi}(z_s)}{\partial y}\frac{\partial z_s}{\partial y}\right] - \left[\bar{\phi}(h)\frac{\partial^2 h}{\partial y^2} - \bar{\phi}(z_s)\frac{\partial^2 z_s}{\partial y^2}\right] \quad \text{(B6)}$$

$$\int_{z_S}^{h} \frac{\partial^2 \bar{\phi}}{\partial z^2} dz = \frac{\partial \bar{\phi}(h)}{\partial z} - \frac{\partial \bar{\phi}(z_S)}{\partial z} \quad \text{(B7)}$$

Considering $\langle \bar{\phi} \rangle = (h - z_S)^{-1} \int_{z_S}^{h} \bar{\phi}(x, y, z)dz$, the vertically integrated potential function, the expression above becomes:

$$\int_{z_S}^{h} \frac{\partial^2 \bar{\phi}}{\partial x^2} dz = \frac{\partial^2}{\partial x^2}\left[\langle \bar{\phi} \rangle \cdot (h - z_S)\right] - 2\left[\frac{\partial \bar{\phi}(h)}{\partial x}\frac{\partial h}{\partial x} - \frac{\partial \bar{\phi}(z_S)}{\partial x}\frac{\partial z_S}{\partial x}\right] - \left[\bar{\phi}(h)\frac{\partial^2 h}{\partial x^2} - \bar{\phi}(z_S)\frac{\partial^2 z_S}{\partial x^2}\right] \quad \text{(B8)}$$

$$\int_{z_S}^{h} \frac{\partial^2 \bar{\phi}}{\partial y^2} dz = \frac{\partial^2}{\partial y^2}\left[\left\langle \bar{\phi} \right\rangle \cdot (h - z_S)\right] - 2\left[\frac{\partial \bar{\phi}(h)}{\partial y}\frac{\partial h}{\partial y} - \frac{\partial \bar{\phi}(z_S)}{\partial y}\frac{\partial z_S}{\partial y}\right] - \left[\bar{\phi}(h)\frac{\partial^2 h}{\partial y^2} - \bar{\phi}(z_S)\frac{\partial^2 z_S}{\partial y^2}\right] \quad \text{(B9)}$$

Similarly, considering the others directions, the Laplacian vertically integrated in the PBL can be finally written as:

$$\begin{aligned} \left\langle \nabla^2 \bar{\varphi} \right\rangle \quad = \quad & (h - z_S)^{-1} \nabla_H^2 \left[\left\langle \bar{\varphi} \right\rangle (h - z_S)\right] \\ & - (h - z_S)^{-1}\left[2\nabla_H h \cdot \nabla_H \bar{\varphi}(h) + \bar{\varphi}(h)\nabla_H^2 h - \frac{\partial \bar{\varphi}(h)}{\partial z}\right] \\ & + (h - z_S)^{-1}\left[2\nabla_H z_S \cdot \nabla_H \bar{\varphi}(z_S) + \bar{\varphi}(z_S)\nabla_H^2 z_S - \frac{\partial \bar{\varphi}(z_S)}{\partial z}\right] \end{aligned} \quad \text{(B10)}$$

Appendix C

Combining both sides of (4) as derived in the Appendixes A (A3) and B (B10)

$$(h - z_S)^{-1}\nabla_H^2\left[\left\langle \bar{\phi} \right\rangle \left(h - z_S\right)\right] - (h - z_S)^{-1}\left[2\nabla_H h \cdot \nabla_H \bar{\phi}(h) + \bar{\phi}(h)\nabla_H^2 h - \frac{\partial \bar{\phi}(h)}{\partial z}\right]$$

$$+ (h - z_S)^{-1}\left[2\nabla_H z_S \cdot \nabla_H \bar{\phi}(z_S) + \bar{\phi}(z_S)\nabla_H^2 z_S - \frac{\partial \bar{\phi}(z_S)}{\partial z}\right] =$$

$$-(h - z_S)^{-1}\left\{\nabla_H \cdot \left[(h - z_S)\left\langle \bar{v}_H^0 \right\rangle\right] - \left[\bar{v}_H^0(h) \cdot \nabla_H h - \bar{w}^0(h)\right] + \left[\bar{v}_H^0(z_S) \cdot \nabla_H z_S - \bar{w}^0(z_S)\right]\right\} \quad \text{(C1)}$$

The first term in the LHS of equation C1 can be rearranged as

$$(h - z_S)^{-1}\nabla_H^2\left[\langle\bar{\phi}\rangle\left(h - z_S\right)\right] =$$

$$(h - z_S)^{-1}\left\{\left(h - z_S\right)\nabla_H^2\langle\bar{\phi}\rangle + 2\nabla_H\langle\bar{\phi}\rangle\cdot\nabla_H\left(h - z_S\right) + \langle\bar{\phi}\rangle\nabla_H^2\left(h - z_S\right)\right\}$$

(C2)

and the result can be substituted in (C1)

$$(h - z_S)^{-1}\left\{\left(h - z_S\right)\nabla_H^2\langle\bar{\phi}\rangle + 2\nabla_H\langle\bar{\phi}\rangle\cdot\nabla_H\left(h - z_S\right) + \langle\bar{\phi}\rangle\nabla_H^2\left(h - z_S\right)\right\}$$

$$- (h - z_S)^{-1}\left[2\nabla_H h\,.\nabla_H\bar{\phi}(h) + \bar{\phi}(h)\nabla_H^2 h - \frac{\partial\bar{\phi}(h)}{\partial z}\right]$$

$$+ (h - z_S)^{-1}\left[2\nabla_H z_S\,.\nabla_H\bar{\phi}(z_S) + \bar{\phi}(z_S)\nabla_H^2 z_S - \frac{\partial\bar{\phi}(z_S)}{\partial z}\right]$$

$$= -(h - z_S)^{-1}\left\{\nabla_H\cdot\left[\left(h - z_S\right)\langle\bar{v}_H^0\rangle\right] - \left[\bar{v}_H^0(h).\nabla_H h - \bar{w}^0(h)\right]\right.$$

$$\left. + \left[\bar{v}_H^0(z_S).\nabla_H z_S - \bar{w}^0(z_S)\right]\right\}$$

(C3)

$$\nabla_H^2\langle\bar{\phi}\rangle = -(h - z_S)^{-1}\nabla_H\cdot\left[\left(h - z_S\right)\langle\bar{v}_H^0\rangle\right]$$

$$-(h - z_S)^{-1}\left[2\nabla_H\langle\bar{\phi}\rangle\cdot\nabla_H\left(h - z_S\right) + \langle\bar{\phi}\rangle\nabla_H^2\left(h - z_S\right)\right]$$

$$+(h - z_S)^{-1}\left[2\nabla_H h\,.\nabla_H\bar{\phi}(h) + \bar{\phi}(h)\nabla_H^2 h - \frac{\partial\bar{\phi}(h)}{\partial z}\right]$$

$$-(h - z_S)^{-1}\left[2\nabla_H z_S\,.\nabla_H\bar{\phi}(z_S) + \bar{\phi}(z_S)\nabla_H^2 z_S - \frac{\partial\bar{\phi}(z_S)}{\partial z}\right]$$

$$+(h - z_S)^{-1}\left[\bar{v}_H^0(h).\nabla_H h - \bar{w}^0(h)\right]$$

$$+(h-z_S)^{-1}\left[\bar{\vec{v}}_H^0(h).\nabla_H h-\bar{w}^0(h)\right]$$

$$-(h-z_S)^{-1}\left[\bar{\vec{v}}_H^0(z_S).\nabla_H z_S-\bar{w}^0(z_S)\right]$$

(C4)

$$\nabla_H^2\langle\bar{\phi}\rangle = -(h-z_S)^{-1}\nabla_H\cdot\left[\left(h-z_S\right)\left\langle\bar{\vec{v}}_H^0\right\rangle\right]+\varepsilon \qquad \text{(C5)}$$

where

$$\varepsilon = -(h-z_S)^{-1}\left\{\left[2\nabla_H\langle\bar{\phi}\rangle\cdot\nabla_H\left(h-z_S\right)+\langle\bar{\phi}\rangle\,\nabla_H^2\left(h-z_S\right)\right]\right.$$

$$-\left[2\nabla_H h\,.\nabla_H\bar{\phi}(h)+\bar{\phi}(h)\nabla_H^2 h-\frac{\partial\bar{\phi}(h)}{\partial z}\right]$$

$$+\left[2\nabla_H z_S\,.\nabla_H\bar{\phi}(z_S)+\bar{\phi}(z_S)\nabla_H^2 z_S-\frac{\partial\bar{\phi}(z_S)}{\partial z}\right]$$

$$-\left[\bar{\vec{v}}_H^0(h).\nabla_H h-\bar{w}^0(h)\right]$$

$$\left.+\left[\bar{\vec{v}}_H^0(z_S).\nabla_H z_S-\bar{w}^0(z_S)\right]\right\}$$

Av. Rio Branco, 124 - 14. Andar
20040-001 Rio de Janeiro RJ - Brazil
Tel. : (55 21) 2221-0438

e-Mail
abcm@domain.com.br